ISSN 2231-4040

Journal of Advanced Pharmaceutical Technology & Research

An Official Publication of Society of Pharmaceutical Education & Research

Vol 2 / Issue 3 / Jul-Sept 2011

www.japtr.org

JAPTR

Medknow Publications

ORIGINAL ARTICLE

Qualitative analysis of controlled release ciprofloxacin/ carbopol 934 mucoadhesive suspension

Subhashree Sahoo,
Chandra Kanti Chakraborti,
Subash Chandra Mishra[1]

Department of Pharmaceutics, Kanak Manjari Institute of Pharmaceutical Sciences, [1]Department of Metallurgical and Materials Engg, National Institute of Technology, Rourkela, Orissa, India

J. Adv. Pharm. Tech. Res.

ABSTRACT

Mucoadhesive polymeric (carbopol 934) suspension of ciprofloxacin was prepared by ultrasonication and optimized with the aim of developing an oral controlled release gastro-retentive dosage form. The qualitative analysis of the formulation was performed by fourier transform infrared spectroscopy (FTIR), Raman spectroscopy, X-ray powder diffraction (XRD), and scanning electron microscopy (SEM) analyses. FTIR (400 cm^{-1} to 4000 cm^{-1} region) and Raman (140 to 2400 cm^{-1} region) Spectroscopic studies were carried out and the spectra were used for interpretation. XRD data of pure drug, polymer and the formulation were obtained using a powder diffractometer scanned from a Bragg's angle (2θ) of 10° to 70°. The dispersion of the particle was observed using SEM techniques. The particle size distribution and aspect ratio of particles in the polymeric suspension were obtained from SEM image analysis. The results from FTIR and Raman spectroscopic analyses suggested that, in formulation, the carboxylic groups of ciprofloxacin and hydroxyl groups of C934 undergo a chemical interaction leading to esterification and hydrogen bonding. The XRD data suggested that the retention of crystalline nature of ciprofloxacin in the formulation would lead to increase in stability and drug loading; decrease in solubility; and delay in release of the drug from polymeric suspension with better bioavailability and penetration capacity. The SEM image analysis indicated that, in the formulation maximum particles were having aspect ratio from 2 to 4 and standard deviation was very less which provided supporting evidences for homogeneous, uniformly dispersed, stable controlled release ciprofloxacin suspension which would be pharmaceutically acceptable.

Key words: Carbopol 934, ciprofloxacin, mucoadhesive suspension

INTRODUCTION

Oral controlled release (CR) dosage forms (DFs) have been developed over the past three decades due to their considerable therapeutic advantages, such as ease of administration, patient compliance, and flexibility in formulation. Incorporation of the drug in a CR - gastro retentive dosage forms (CR-GRDF) can remain in the gastric region for several hours which would significantly prolong the gastric residence time of drugs and improve their bioavailability, reduce drug wastage, and enhance the solubility of drugs.[1] Several approaches are currently used to prolong gastric retention time. Considering the goals of controlled drug delivery,[2] polymeric bioadhesive delayed gastric emptying devices have been explored in the present study.

Ciprofloxacin (Cipro) is a second generation fluoroquinolone antibacterial [Figure 1]. It shows low solubility in aqueous solution and a high rate of absorption from the stomach. It is likely to be precipitated out of solution upon entry into the small intestine where the pH is alkaline. The desire is for a dosage form that will provide a drug at a sustained, constant level in solution in both acidic and basic pH conditions of the gastro intestinal tract (GIT) over the entire transit

Address for correspondence:
Mrs. Subhashree Sahoo,
Department of Pharmaceutics, Kanak Manjari Institute of Pharmaceutical Sciences, Rourkela - 769 015, Orissa, India.
E-mail: subha77t@yahoo.co.in

Access this article online

Quick Response Code:

Website: www.japtr.org

DOI: 10.4103/2231-4040.85541

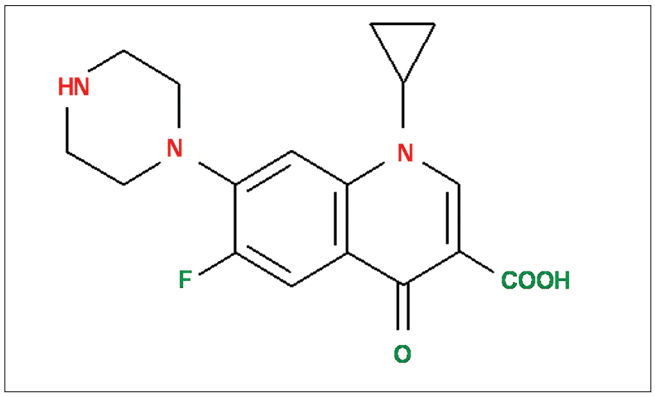

Figure 1: Chemical structure of ciprofloxacin

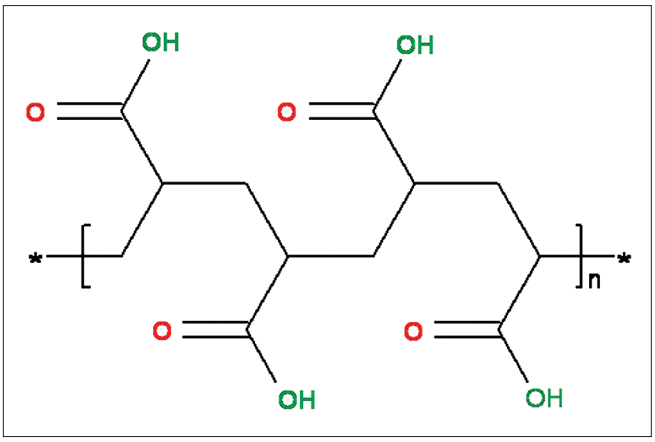

Figure 2: Chemical structure of carbopol polymer

period. For this reason, dosage forms that incorporate low solubility drugs provide a major challenge for sustained release developers.[3]

Carbopol 934 (C934) is a mucoadhesive, biodegradable and environmentally responsive carbopol polymer and is considered as 'smart gels'.[4,5] It consists of chains of polyacrylic acid having cross linking agent, allyl ethers of sucrose (allylsucrose) [Figure 2].[6,7] It has recently attracted considerable interest in the field of drug delivery as a means of providing an on-off release by shrinking and swelling in response to change in pH.[8,9] The polymer can protect a drug from its physiological environment by improving its stability *in vivo*.[10]

C934 may form a complex with the low solubility drug like ciprofloxacin. The interaction between Cipro and C934 can be determined by several methods such as Fourier transform infrared (FTIR) spectroscopy, Raman spectroscopy, etc. To know the different functional groups and highly polar bonds of both pure Cipro and C934 and their chemical interactions in the mucoadhesive suspension, FT-IR analysis was conducted. However, their backbone structures and symmetric bonds were checked by Raman spectroscopy. Although it is known that Raman and FTIR are complementary vibrational spectroscopic techniques, there are band intensity differences between the two techniques. That is why both FTIR and Raman spectroscopic analyses were conducted.

The X-ray diffraction (XRD) method has become one of the most useful tools for qualitative characterization of crystalline compounds both in the formulation and in the pure form of the drug.[11] It is known that increased dissolution rate and delayed release of drug from dosage forms occur with increase in crystallinity.[12,13] XRD study is important because any change in the morphology of polymers or in the crystalline state of active ingredients in the final product, resulting from the manufacturing process, can influence a drug's bioavailability.[14]

The particle size distribution (PSD) and aspect ratio (AR) of particles in the suspension are obtained from scanning electron microscopic (SEM) analysis.[15-17] The PSD and AR distribution and degree of dispersion in the suspension give insights even into the stability relating to the modification of mechanical properties, particle-matrix interaction, polymer and drug crystallinity and the overall structure of the suspension.[15,18,19]

Therefore, to obtain more detailed information about chemical interaction between ciprofloxacin and C934, FTIR and Raman analyses were carried out.[20,21] Moreover, considering the bioavailability, stability and degree of dispersion of the particles present in the formulation, XRD and SEM analyses were conducted.[5,8,9,18,19] In the present investigation, we performed FTIR analysis, Raman spectroscopy, XRD and SEM studies because all the positive aspects of different qualitative analyses were taken into account.

MATERIALS AND METHODS

Materials

The following materials were used: Ciprofloxacin hydrochloride was obtained from Dr. Reddy's Lab, Hyderabad, India, as a gift sample. C934, pluronic F68 and soya lecithin were purchased from Himedia Laboratories Pvt. Ltd., (Mumbai) India. Citric acid, sodium citrate, glycerol, methyl praraben, propyl paraben, sorbitol solution (Indian Pharmacopoeia) and sucrose were kindly supplied by Cosmo Chem. Laboratory, (Pune) India. Ultra pure water was obtained from a millipore milli-Q UV water filtration system.

Methods

Formula for preparation of mucoadhesive suspension

Ciprofloxacin 6%
Carbopol 934 5%
Pluronic F 68 5%
Soya lecithin 1%

Sorbitol Solution (80%) 7.2%
Glycerin 0.8%
Methyl paraben sodium 0.015%
Propyl paraben sodium 0.08%
Simple syrup IP 40%
Purified water q.s. up to 100 ml

Preparation of formulation

Preparation of bulk A

In a beaker, 6 ml water was taken and it was heated up to 80°C. Sucrose (10 gm) was added to that water with continuous stirring. The temperature was monitored in such a way so that it does not fall below 70°C till the sucrose was completely dissolved. The prepared syrup was cooled properly at room temperature and kept aside overnight. Syrup was filtered using 120 mesh nylon cloth.

Preparation of bulk B

Five milliliters of ultra pure water was taken in a beaker to which 1.8 ml of sorbitol solution and 0.2 ml glycerin were added. The mixture was stirred properly. Pluronic F 68 (5%), soya lecithin (1%) and C934 (5%) in w/w of drug were added to this solution with continuous stirring.

Preparation of mucoadhesive suspension and ultrasonication

Five milliliters of water was taken in another beaker to which 1.25 gm of Cipro was added. To the drug suspension, the bulk B and bulk A were added with continuous stirring. Methyl paraben sodium (0.015%w/v) and propyl paraben sodium (0.08%w/v) were added as preservatives. The volume was made up to 25 ml by ultra pure water. The pH was adjusted to 5.5. Homogenization was carried out for at least 20 min by ULTRASONIC HOMOZENIZER LABSONIC^{R} M (SARTORIUS), having operating frequency 30 KHZ and line voltage 230 V/50 HZ, using the probe made up of titanium of diameter 7 mm and length 80 mm. The setting knob "cycle" was adjusted to 0.8 indicating sound was emitted for 0.8 s and paused for 0.2 s. In this manner, we could expose our sample with 100% amplitude, while reducing the heating effect to 80%. This LABSONIC^{R}M generates longitudinal mechanical vibrations with a frequency of 30,000 oscillations/s (30 KHZ). The probes bolted to the sound transducer were made of high-strength titanium alloys, built as $\lambda/2$ oscillators. It amplified the vertical oscillation and transferred the ultrasonic energy via its front surface with extremely high power density into the sample that was to be subjected to ultrasonic waves. In our study, stress applied was a sound wave and in addition, mild rise in temperature of the sample occurred during ultrasonication which helped in the homogenization of the suspension. Some portion of the homogenized suspension was kept for Raman spectroscopic analysis and SEM study. The remaining portion of the suspension was sprayed on to an aluminum slip with the aid of an atomizer. The fine droplets were dried overnight at room temperature and the solid samples were then collected and powdered. The sample was then divided into two parts - one part was for FTIR analysis and the other part was used for XRD study.

Fourier Transform Infrared Spectroscopy

FT-IR analysis was performed by FTIR spectrophotometer interfaced with infrared (IR) microscope operated in reflectance mode. The microscope was equipped with a video camera, a liquid nitrogen-cooled mercury cadmium telluride (MCT) detector and a computer controlled translation stage, programmable in the x and y directions. Solid powder samples were oven dried at around 30°C, finely crushed, mixed with potassium bromide (1:100 ratio by weight) and pressed at 15000 psig (using a Carver Laboratory Press, Model C, Fred S. carver Inc., WIS 53051) to form disc. The detector was purged carefully using clean dry nitrogen gas to increase the signal level and reduce the moisture. The spectra were collected in the 400 cm^{-1} to 4000 cm^{-1} region with 8 cm^{-1} resolution, 60 scans and beam spot size of 10 μm-100 μm.[22-24] The FTIR imaging in the present investigation was carried out using a Perkin Elmer spectrum RX.

Raman Spectroscopic Analysis

The Raman system R-3000 instrument (Raman systems Inc. (Dunedin) USA), a low resolution portable Raman spectrometer using a 785 nm solid state diode laser was adjusted to deliver 250 mw to the sample having spectral resolution 10 cm^{-1} and 12 v dc/5A power supplies and universal serial bus (USB) connectivity. The solid powder samples i.e., both pure drug and polymers were enclosed in plastic poly bags and tested directly. For our study, the fiber optic sampling probe was directly dipped into the formulation (prepared as per the above mentioned procedure) to collect the spectra at room temperature. The interference of the outside light was also prohibited to prevent photon shot noise. The spectra were collected over the wave number range from 140 to 2400 cm^{-1}.

X-ray Diffractometry

XRD measurements were obtained using the Philips X'Pert on powder diffraction system (Philips Analytical, (Almelo) The Netherlands) equipped with a vertical goniometer in the Bragg-Brentano focusing geometry. The X-ray generator was operated at 40 kV and 50 mA, using the CuKα line at 1.54056 Å as the radiation source. The powdered specimen was packed and prepared in a specimen holder made of glass. In setting up the specimen and apparatus, co-planarity of the specimen surface with the specimen holder surface and the setting of the specimen holder at the position of symmetric reflection geometry were assured. The powders were passed through a 100 mesh sieve and were placed into the sample holder by the side drift technique.[25] In order to prepare a sample for analysis, a glass slide was clipped up to the top face of the sample holder so as to form a wall. Each powder was filled into the holder and tapped gently. Each sample was scanned

from 10° to 70° (2θ) and in stage sizes of 0.020; count time of 2.00 s, using an automatic divergence slit assembly and a proportional detector. The samples were scanned at 25°C. Relative intensities were read from the strip charts and corrected to fix slit values.

Scanning Electron Microscopy

In order to examine the particle surface morphology and shape, SEM was used. The mucoadhesive suspension (as mentioned above) was sprayed on to an aluminum slip with the aid of an atomizer. The fine droplets were dried overnight and it was used for SEM analysis.[26] The samples were given a conductive coating (using Pt, of about 600 Å thick) using sputter ion coater and examined with SEM (JEOL JSM-6480LV) equipped with a backscattered electron detector for imaging and Energy-Dispersive X-ray Analysis (EDXA) for elemental analysis. In this method, a focused electron beam is scanned over the sample in parallel lines. The electrons interact with the sample, producing an array of secondary effects, such as back-scattering, that can be detected and converted into an image. The image can then be digitalized and presented to an image analyzer which uses complex algorithms to identify individual particles and to record detailed information about their morphology. Then particle size can be determined with a program, such as image tool, or annotate either automatically or manually. Here, manual determination is preferred, because sometimes the particle boundaries are indistinct and the software may interpret them incorrectly. The PSDs reflect the statistical result from all sections for each sample. As these are rod like particles, the ARs of rod-like particles are evaluated by comparing the particle size distribution data derived from SEM analysis following the techniques described by Jennings and Parslow.[18] Length/width ratios are satisfactorily determined by the AR value.

RESULTS

FTIR Analysis

In the FTIR spectra of Cipro, one prominent characteristic peak was found between 3500 and 3450 cm^{-1} [Figure 3a] and was assigned to an OH stretching vibration (intermolecular hydrogen bonding). Another band at 3000-2950 cm^{-1} represented alkenes and aromatic C-H stretching, mainly stretching vibration of aromatic enes. The bands at 1750 to 1700 cm^{-1} indicated carbonyl C = O stretching, i.e., $\upsilon_{C=O}$ while the peak at 1650 to 1600 cm^{-1} was assigned to quinolones. The bands at the 1450 to 1400 cm^{-1} represented υ_{C-O} and the peaks at 1300 to 1250 cm^{-1} suggested bending vibration of O-H group which indicated the presence of carboxylic acid. In addition, a strong absorption peak between 1050 and 1000 cm^{-1} was assigned to C-F group [Table 1a].[23,27]

For C934, its FTIR spectra showed a peak in the 3000-2950 cm^{-1} range, representing OH stretching vibration, i.e., υ_{O-H} and intramolecular hydrogen bonding [Figure 3b]. The prominent peak between 1750 and 1700 cm^{-1} was assigned to carbonyl C = O stretching band i.e., $\upsilon_{C=O}$ while the peak at 1450 to 1400 cm^{-1} was for $\upsilon_{C-O}/\delta_{O-H}$. The band at 1250 to 1200 cm^{-1} suggested υ_{C-O-C} of acrylates.[22,23] The ethereal crosslinking, indicated by the prominent peak at 1160 cm^{-1} represented a stretching vibration of υ_{C-O-C} group. The band between 850 and 800 cm^{-1} suggested out of plane bending of C = CH, i.e., bending vibration of aromatic enes [Table 1b].[23,28]

In the FTIR spectra of the formulation, the prominent band between 3550 and 3500 cm^{-1} was assigned to υ_{O-H} and hydrogen bonding by single bridge [Figure 3c]. While the peak in the range of 3450 to 3400 cm^{-1} was assigned to polymeric υ_{O-H} and hydrogen bonding, the band between 2650 and 2600 cm^{-1} represented the υ_{O-H}, i.e., strong hydrogen bonding. The band from 1650 to 1600 cm^{-1} was assigned to $\upsilon_{C=O}$ i.e., carbonyl stretching vibration. A prominent peak at 1450 cm^{-1} (w) was for $\upsilon_{C-O}/\delta_{O-H}$. The band from 1300 to 1250 cm^{-1} was assigned to υ_{C-O-C} of acrylates. The peak between 1100 and 1000 cm^{-1} represented υ_{C-F} groups, while the band at 800 cm^{-1} indicated the meta distribution of δ_{Ar-H} group [Table 1c].[22,23]

Raman Spectroscopy

In case of Cipro, the prominent Raman shifts were observed at 484.22, 771.47, 1411.63, and 1655.11 cm^{-1} [Figure 4a]. The Raman shifts at 484.22 cm^{-1} indicated strong bending vibration of C-C of the aliphatic chain of cyclopropyl group and C-N stretching vibration of piperazinyl group.[30-32] The band at 771.47 cm^{-1} represented the symmetric stretching vibration of C-F group.[29,30-32] The

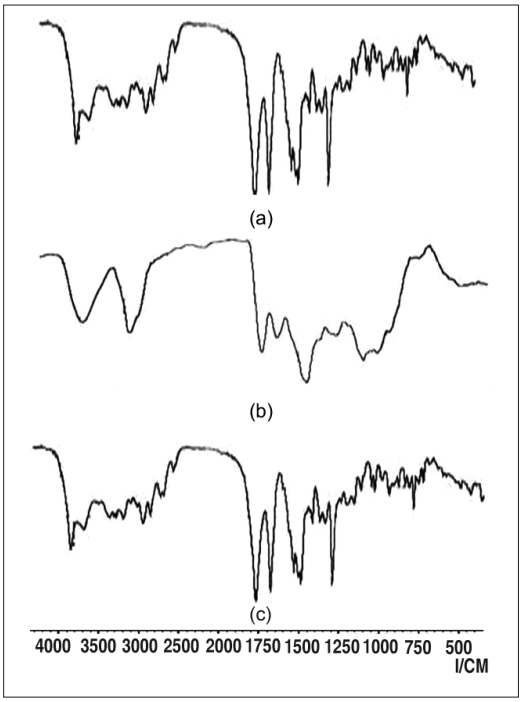

Figure 3: FTIR spectra of (a) Cipro, (b) C934 and (c) Mucoadhesive suspension

peak at 1411.63 cm^{-1} was due to symmetric stretching vibration of O-C-O group of carboxylic acid and methylene deformation mode of the piperazinyl group.[33] A band at 1655.11 cm^{-1} was for symmetric stretching of the carbonyl group $\upsilon_{C=O}$ of the pyridone moiety, the stretching vibration of (C-C) aromatic ring chain.[27] In addition, it (peak at 1655.11 cm^{-1}) also indicated the $N^{+}H_2$ scissoring of piperzinyl group [Table 2a].[27,30,33-36]

Similarly, the characteristic prominent Raman bands for C934 were observed at 350, 514.31, 872.69, and 1335.03 cm^{-1} [Figure 4b]. The band at 872.69 cm^{-1} was due to the stretching vibration of C-O-C for acrylates and carboxylic acid. The Raman band at 1335.03 cm^{-1} was assigned to the symmetric vibration of O-C-O of acids [Table 2b].[30]

The characteristics Raman peaks of formulation containing both Cipro and C934 were observed at 334.75, 812.50, 906.25, 1369.4, 1562.5, and 1703.12 cm^{-1} [Figure 4c]. The band at 812.50 cm^{-1} was assigned to symmetric stretching vibration of C-O-C for acrylates and esters. The Raman shifts at 906.25 cm^{-1} was due to the asymmetric stretching vibration of C-O-C. The band at 1703.12 cm^{-1} was the characteristic of stretching vibration of carbonyl group of esters [Table 2c].[36]

Table 1: Comparative study of FT-IR peaks

(a) Prominent FT-IR Peaks of ciprofloxacin		
Peaks (cm^{-1})	**Groups**	**Peak assignment**
3500-3450	Hydroxyl group	O-H stretching vibration, intermolecular H-bonded
3000-2950	Aromatics, cyclic enes	υ = CH and Ar-H
1750-1700	CO group of acid	C = O stretching vibration
1650-1600	Quinolines	δN-H bending vibration
1450-1400	Carbonyl group	υC-O
1300-1250	Hydroxyl group	δO-H bending vibration
1050-1000	Fluorine group	C-F stretching
(b) Prominent FT-IR peaks of C934		
3000-2950	Hydroxyl group	O-H stretching vibration, intramolecular H-bonded
1750-1700	C = O group of acids	υC = O stretching vibration
1450-1400	Carbonyl group of acids	C-O stretching vibration
1250-1200	Acrylates	C-O-C stretching vibration
1160	Ethereal C-O-C group	Stretching vibration of C-O-C group
850-800	Aromatics and enes	= C-H out of plane bending vibration
(c) Prominent FT-IR peaks of mucoadhesive suspension		
3550-3500	Hydroxyl group	H -bonding by single bridge
3450-3400	Polymeric OH groups	υO-H, H-bonding
2650-2600	Strong H-bonding	O-H stretching vibration
1650-1600	O-C-O group of acid	υ_{as} stretching vibration of O-C-O group
1450	O-C-O group of acid	υ_{s} stretching vibration of O-C-O group
1300-1250	Acrylates and esters	C-O-C stretching vibration
1100-1000	C-F groups	υC-F
800	Aromatic m-distribution	δAr-H

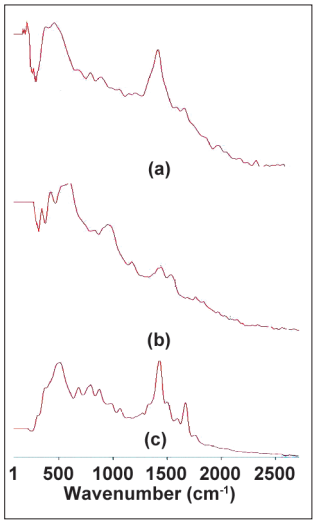

Figure 4: Raman Shifts of (a) Cipro, (b) C934 and (c) Mucoadhesive suspension

Table 2: Comparative study of Raman shifts

(a) Prominent Raman shifts of ciprofloxacin	
Raman shifts (cm^{-1})	**Functional groups/vibration**
484.22	Strong δ(CC) aliphatic chain
771.47	υ(CC) alicyclic chain vibration
1411.63	υ_{s}O-C-O
1655.11	υ_{s} of C = O group of pyridone moiety
(b) Prominent Raman shifts of C934	
350	Strong δ(CC) aliphatic chain
514.31	C-C-O bending vibration
872.69	υ(C-O-C) of acrylates
1335.03	υ_{s}O-C-O of acids
(c) Prominent Raman shifts of mucoadhesive suspension	
334.75	δ(CC) aliphatic chain
812.5	υ(C-O-C) of acrylates/esters
906.25	υ(C-O-C) asymmetric
1369.4	υ_{s}O-C-O
1562.5	υ_{as}O-C-O
1703.12	υC = O medium

XRD Study

All the high intensity peaks (relative intensity) observed in the XRD pattern of the pure Cipro were compared with its mucoadhesive polymeric suspension [Tables 3 and 4]. Both the polymeric suspension and pure Cipro were found to show similar XRD patterns [Figure 5]. Identification of the molecular structure from its powdered diffraction pattern is based upon the position of peaks and their relative intensities. Each XRD pattern is characterized by the interplanar d-spacing and the relative intensities (I/I_0) of the three strongest peaks in the pattern under the Hanawalt system. The relative intensities and heights of three prominent peaks of our formulation were less than those of pure Cipro [Table 3]. The entire diffractograms, rather than selected peaks, are still required to distinguish the samples. Hence, comprehensive Å and I/I_0 data, presented in Table 4, clearly identify Cipro even in the polymeric composites.

SEM Analysis

The length/width ratios of individual particles can satisfactorily determine their ARs. PSD analysis of the formulation showed different ranges of length of particles along with their frequencies [Table 5, Figure 6]. While within 0-5 μm range no particle was found, maximum number of particles was observed within 10-15 μm. In case of formulation, maximum AR frequency was found from 4 to 6 [Table 6].

DISCUSSION

When FTIR radiation falls on a molecule, it may be absorbed, reflected or transmitted. Absorption leads to the FTIR spectrum, while reflection leads to scattering which is utilized in Raman spectroscopy.[22] In addition, IR absorption of the functional groups may vary over a wide range. However, it has been found that many functional groups give characteristics IR absorption at specific narrow frequency range.[22,23]

IR absorption of the functional groups may vary over a wide

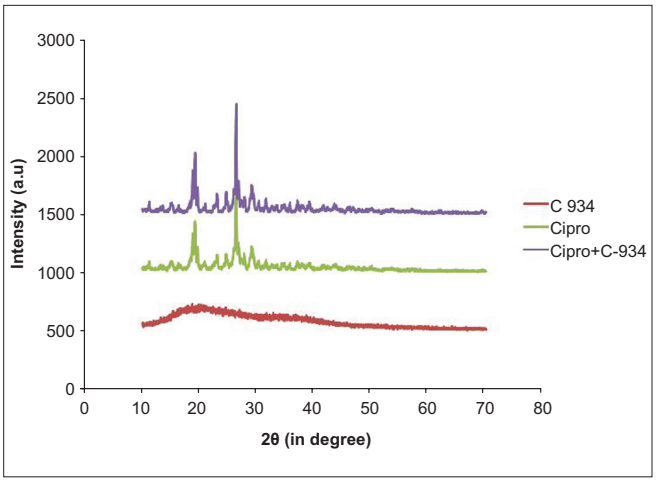

Figure 5: X-ray diffraction patterns of C934, Cipro and mucoadhesive suspension

Table 3: Lattice spacing (Å) and relative intensities (I/I_0) (based on the Hanawalt System) of the three strongest peaks in the diffractograms of Cipro and mucoadhesive suspension

Ciprofloxacin				Mucoadhesive suspension			
2θ	Å	I/I_0	H	2θ	Å	I/I_0	H
19.22	4.61	54.85	900	19.21	4.62	56.85	792
26.39	3.37	100	1642	26.39	3.38	100	1393
29.16	3.06	28.47	467	29.16	3.06	29.45	401

Table 4: Lattice spacing (Å) and relative intensities (I/I_0) of all the identifiable peaks in the diffractograms of ciprofloxacin and mucoadhesive suspension

Sample no.	Ciprofloxacin		Mucoadhesive suspension	
	Å	I/I_0	Å	I/I_0
01	7.86	9.10	7.87	9.34
02	5.50	5.37	6.71	5.42
03	5.85	10.98	6.48	5.59
04	5.42	5.76	5.85	12.78
05	4.71	38.92	5.42	8.28
06	4.61	54.85	4.71	41.26
07	4.51	22.06	4.62	56.85
08	4.23	7.98	4.51	26.25
09	3.96	5.97	4.24	10.51
10	3.86	18.01	3.86	19.51
11	3.60	19.61	3.60	20.74
12	3.37	100.00	3.37	100.00
13	3.31	27.18	3.20	17.86
14	3.26	13.26	3.06	29.45
15	3.20	15.74	2.95	12.41
16	3.10	28.47	2.83	12.58
17	2.95	11.48	2.74	7.35
18	2.83	13.70	2.68	6.98
19	2.74	6.81	2.58	8.76
20	2.68	7.16	2.51	8.71
21	2.61	5.69	2.42	11.77
22	2.58	8.94	2.37	8.29
23	2.51	9.22	2.30	9.66
24	2.42	11.24	2.17	7.59
25	2.37	7.84	2.13	5.21
26	2.30	10.40	2.07	7.75
27	2.27	4.49	1.98	5.46
28	2.23	2.69	1.94	5.33
29	2.17	7.79	1.90	3.84
30	2.13	5.80	1.86	3.09
31	2.08	7.46	1.83	4.27
32	2.06	7.29	1.71	3.23
33	1.98	5.70	1.61	2.20
34	1.94	5.03	1.50	0.66

2θ: Angle of incidence of the X-ray beam; d: Distance between adjacent planes of atoms; I/I_0: Relative intensities

Table 5: Particle size distribution of mucoadhesive suspension

L (μm)	f	c.f	m	(m – A)/d (m – 17.5)/d	fd	Ā	fd^2	σ	C.V.
0-5	0	0	2.5	–3	0	13.24	0	5.035	38%
5-10	14	14	7.5	–2	–28		56		
10-15	26	40	12.5	–1	–26		26		
15-20	8	48	17.5	0	0		0		
20-25	4	52	22.5	1	4		4		
25-30	2	54	27.5	2	4		8		
	N = 54				Σ fd = –46		Σ fd^2 = 94		

L: Length of each particle; f: Frequency; c.f: Cumulative frequency; m.p (m): Midpoint; A: Assumed mean; i: Class interval; d: Deviation of midpoint from assumed mean; Ā: Actual mean; σ: Standard deviation; C.V.: Coefficient of variation; N: Total number of particles taken into consideration

Table 6: Aspect ratio analysis of mucoadhesive suspension

A.R.(L/D)	f	c.f	m	(m-A)/i or (m-7)/i = d	fd	Ā	fd^2	σ	C.V.
0-2	4	4	1	-3	-12		36		
2-4	15	19	3	-2	-30	5.35	60	2.67	49.9%
4-6	19	38	5	-1	-19		19		
6-8	8	46	7	0	0		0		
8-10	6	52	9	1	6		6		
10-12	1	53	11	2	2		4		
12-14	0	53	13	3	0		0		
14-16	1	54	15	4	4		16		
	N = 54				Σ fd = –49		Σ fd^2 = 141		

L: Length of each particle; f: Frequency; c.f: Cumulative frequency; m.p (m): Midpoint; A: Assumed mean; i: Class interval; d: Deviation of midpoint from assumed mean; Ā: Actual mean; σ: Standard deviation; C.V.: Coefficient of variation; N: total number of particles taken into consideration; D: Width of each particle

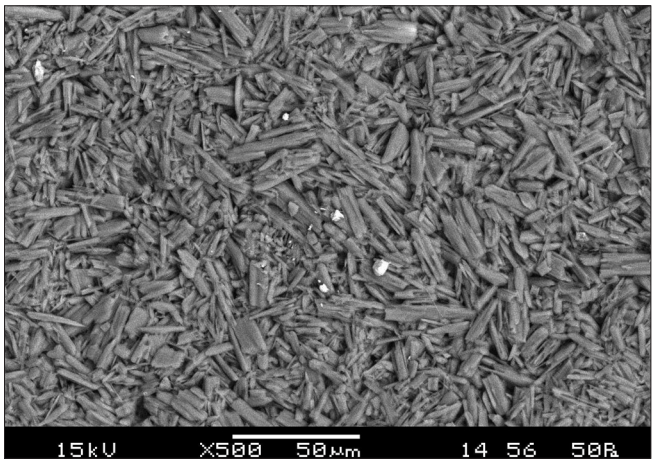

Figure 6: SEM of mucoadhesive suspension

range. However, it has been found that many functional groups give characteristics IR absorption at specific narrow frequency range.[26,32,37]

In case of FTIR spectra of Cipro, prominent peaks for $\upsilon_{C\text{-}O}$/ $\delta_{O\text{-}H}$ and $\upsilon_{C=O}$ indicated the presence of -CO-, -CHO and -COOH groups [Figure 3a]. The presence of above groups can be confirmed by fermi resonance bands for -CHO, $\upsilon_{C\text{-}O\text{-}C}$ bands for esters and absence of these two for ketones. This suggested the existence of -COOH group in Cipro molecule [Table 1a].

In case of FTIR spectra of C934, there were prominent peaks for intramolecular hydrogen bonding, υ_{OH} stretching vibration, carbonylic C = O and C-O stretching vibration and stretching vibration for the C-O-C which confirmed the presence of acrylates [Figure 3b]. The peak for out of plane bending vibration of = C-H was found between 850 and 800 cm^{-1} [Table 1b].

While comparing the FTIR spectra among the pure Cipro and C934, and the formulation containing both Cipro and C934, it is clear that the band position of C = O group has been affected by esterification and conjugation involving C = O group. Here, the stretching vibration of C = O in pure Cipro was found from 1750 to 1700 cm^{-1} which was lowered to 1650-1600 cm^{-1} in this formulation. It might be due to formation of β-ketoesters [Figure 3]. The FTIR peaks assigned to $\upsilon_{C\text{-}O}$ and $\upsilon_{C\text{-}O\text{-}C}$ representing acrylates and esters confirm the esterification between polymeric OH group and -COOH group of drug (Cipro). The stretching vibration of C-F group remains nearly unaltered. Another probability of interaction is hydrogen bonding i.e., intermolecular hydrogen bonding due to prominent FTIR peaks between 3550 and 3500 cm^{-1}, 3450 and 3400 cm^{-1}, and 2650 and 2600 cm^{-1} represent single bridge O-H…O, polymeric O-H.O-H…O-H and strong hydrogen bonding, respectively. The hydrogen bonded -OH stretching vibration occurred over a wide range, 3550-2600 cm^{-1}. In case of intramolecular hydrogen bonding, FTIR bands are

sharp while in intermolecular hydrogen bonding bands are broad. However, it is less broad than which is required for chelation. The bending vibration of O-H group gave medium to strong bands in the region around 1450 cm^{-1}. The FTIR peak at 800 cm^{-1} gave the probability of out of plane bending of -ene bond and m-substitution of $\delta_{Ar\text{-}H}$ hydrogen atom [Table 1c].[22,23,26]

The C = O group of drug lowers the stretching vibration of C = O frequency indicating deprotonation and probably interaction of the said carboxylic C = O moiety with the polymer. However, a definitive conclusion about the keto group in the bonding to the polymer can be deduced because the corresponding band found from 1650 to 1600 cm^{-1} is due to the probability of formation of β-ketoesters.[38] From the above data, it can be inferred that the carboxylic group of Cipro undergoes the interaction with the polymer as would be expected chemically. Thus, the nitrogen atoms aren't likely to be involved in binding or the interaction. The nitrogen atom of the quinolone ring, 1-ortho to fluorine, is less electron rich due to electron deficient fluoroquinolone ring. In addition, cyclopropyl and piperazinyl groups sterically hinder the reaction. The possibility of involvement of imino moiety of the piperazinyl group is also less prominent due to intense OH stretching vibration. The bands in the region 3500-2700 cm^{-1} can be assigned to the asymmetric and symmetric stretching vibrations of the OH groups of the inner and outer sphere of polymer. The shift in the characteristic bands of the FTIR spectra suggests change of their intensity leading to the appearance of several absorbance bands of the asymmetric and symmetric stretching vibrations and overtone of the deformation vibrations. This indicates the confirmation of the hydrogen bonding.[25] By comparing the FTIR spectra among the pure drug, carbopol polymer (C934) and the formulation containing both drug and polymer, the FTIR peak of Cipro from 1750 to 1700 cm^{-1} was not detected in the mucoadhesive system probably due to interaction with polymer. The missing peak that has been replaced with two very strong characteristic bands in the range of 1650-1600 cm^{-1} and at 1450 cm^{-1} are assigned to $\upsilon_{(O\text{-}C\text{-}O)}$ asymmetric and symmetric stretching vibrations, respectively.[23,26] The difference Δ [$\upsilon_{(CO2)asym}$-$\upsilon_{(CO2)sym}$] is a useful characteristic for determining the involvement of the carboxylic group of Cipro. The Δ value for the interaction falls in the range of 183-250 cm^{-1} indicating the deprotonation of the carboxylic acid group and interaction between the drug and polymer [Table 1].[33]

In case of Raman spectra of Cipro, the Raman band at 771.47 cm^{-1} was assigned to the stretching vibration of cyclopropyl group. The presence of carboxylic acid group is confirmed by $\upsilon_{O\text{-}C\text{-}O}$ and $\upsilon_{C=O}$ groups vibration at 1411.63 cm^{-1} and 1655.11 cm^{-1}, respectively [Table 2a].

By comparing the Raman spectra of pure drug with the drug incorporated in the carbopol suspension, the peak at 1411.63 cm^{-1} was assigned to the $\upsilon_{s\ O\text{-}C\text{-}O}$, is not prominent. While both symmetric and asymmetric stretching vibrations of O-C-O group are found in the suspension containing C934. The Raman peak for stretching vibration of C = O is prominent in the suspension. From this it is clear that there is an esterification reaction between Cipro and carbopol polymer [Table 2]. The results of both FTIR and Raman spectra indicate that both the spectra show prominent peaks for the stretching vibration of O-C-O and C = O groups which prove the formation of the esters between the drug and polymer. Moreover, both the intermolecular and polymeric hydrogen bondings are also prominent from the FTIR spectra of the formulation.

Tables 3 and 4 give the XRD data obtained for the pure Cipro and its polymeric suspension with C934 in terms of the lattice spacing and the relative peak intensities. Most of the characteristic peaks in the diffraction patterns are generally prominent and sharp, so measurement of the angles and d-values is accurate.

From the XRD patterns of C934, it is clear that the polymer is fully crystalline in nature as there are sharp and prominent peaks [Figure 5]. Table 3 confirms that the three prominent peaks of pure Cipro and its mucoadhesive suspension do not have similar d-spacing corresponding to identical 2θ values. As the d-spacing of the prominent XRD peaks of pure Cipro is changed in the polymeric composites, it may be concluded that there is interaction between Cipro and C934 [Figure 5]. However, Cipro can be easily distinguished even in the formulation. Moreover, since relative intensities of the peaks are decreased in formulation, crystallinity is also reduced in the composites as compared with pure Cipro. This decrease in relative intensities of these peaks appears to be due to change in atomic densities in that particular plane of crystal lattice. From this, we may predict that there is a little bit change in the orientation of crystal lattice due to incorporation of some extra atoms into it which may be due to hydrogen bonding and esterification.

As we know the standard deviation measures the absolute dispersion (or variability of a distribution), a small standard deviation indicates a high degree of uniformity of the observations as well as homogeneity of a series.[39] The series in which co-efficient of variation is less is said to be less variable and more consistent, uniform, stable, and homogeneous. From PSD study it has been found that maximum particle size of the formulation is within the pharmaceutically acceptable limit [Table 5].[40] From Table 5, it is clear that the maximum particle size range for formulation containing Cipro and C934 is between 10 and 15 μm. As these are rod like particles, AR has been calculated. From the statistical interpretation, it has been found that ARs in the formulation containing Cipro and C934 are homogeneous, consistent, and stable with lesser standard deviation [Table 6]. The mean particle size and AR values of the formulation (13.24 μm and 5.35, respectively)

show a correlation between the particle size, particle shape, and stability properties, giving confidence in the usefulness of SEM for characterizing such type of formulations.[41,42] The morphologies and mechanical properties of the formulation impart SEM sectioning and imaging which can allow direct measurement of PSD and AR of particles embedded in polymeric suspension. The SEM-derived information correlated well with the mechanical properties of the present formulation. From the above SEM image analysis, it is expected that the formulation containing Cipro and C934 is having better bioavailability and penetration capacity, as maximum particles are of AR values between 2 to 4.[43] From the AR analysis, it can be said that the formulation is more stable because it has lesser standard deviation. Hence, it indicates that the particles in the formulation are uniformly dispersed.

CONCLUSION

On the basis of the above interpretation, it can be concluded that by preparing mucoadhesive suspension of Cipro with C934 following a novel method of ultrasonication, there is a very good interaction between the carboxylic group of drug and hydroxyl group of the polymer. This leads to the esterification and intermolecular hydrogen bonding,[44] by virtue of which a stable mucoadhesive suspension would be produced. From the XRD data supported by FTIR analysis, it appears that the crystalline form of pure Cipro under the experimental conditions resulted in little change in crystal habit of the drug. Moreover, size of the crystals was significantly influenced by intermolecular hydrogen bonding and esterification between Cipro and C934. The retention of crystallinity nature of the drug in the formulation may lead to increase in stability, decrease in solubility, and delay in release of the drug from polymeric suspension. This may result in CR action of the formulation. From the SEM image analysis, it may be concluded that the formulation containing Cipro and C934 is having uniform dispersion of particles and stability which may lead to better bioavailability and penetration capacity than conventional dosage forms. The utility of the present work may be improved if the delivery rate, biodegradation, and site-specific targeting of such as mucoadhesive suspension would be properly monitored and controlled.

REFERENCES

1. Garg R, Gupta GD. Progress in controlled gastroretentive delivery systems. Trop J Pharm Res 2008;7:1055-66.
2. Gupta SK, Gupta U, Omray LK, Yadav R, Soni VK. Preparation and characterization of floating drug delivery system of acyclovir. Int J Appl Pharm 2010;2:7-10.
3. Chang DL, Jasmine EH, Pollock-Dove C, Patrick SLW 2006, (WO/2006/007354) A drug/polymer complex, preferably ciprofloxacin/HPMC, Its method of manufacturing using Lyophilisation and Its use in an Osmotic Device; Available from: http://www.wipo.int/pctdb/en/wo.jsp?WO=2006007354andIA=US2005020356andDISPLAY=DESC, [Last accessed on 2010 Aug 12].
4. Qiu Y, Park K. 2001. Environment-sensitive hydrogels for drug delivery. Adv Drug Deliv Rev 2001;53:321-39.
5. Bettini R, Colombo P, Peppas NA. Solubility effects on drug transport through pH-sensitive, swelling-controlled release systems: Transport of theophylline and metoclopramide monohydrochloride. J Control Release 1995;37:105-11.
6. Hosmani AH. Carbopol and its Pharmaceutical Significance: A Review; Available from: http://www.pharmainfo.net/reviews/carbopol- and-its-pharmaceutical significance-review, [Last accessed on 2011 Feb 15].
7. Cruz AP, Rodrigues PO, Cardoso TM, Silva MA. Mechanical and imaging studies of hydrophilic matrices formed by Polymeric Blends of HPMC and carbopol. Am J Pharm 2007;26:171-8.
8. Galaev IY, Mattiasso B. 'Smart' polymers and what they could do in biotechnology and medicine. Trends Biotechnol 1999;17:335-40.
9. Jeong B, Gutowska A. Stimuli-responsive polymers and their biomedical applications. Trends Biotechnol 2001;20:305-11.
10. Guo JH. Carbopol® Polymers for pharmaceutical drug delivery applications drug delivery technology;. Available from: http://www.drugdeliverytech.com/ME2/dirmod.asp?sid=4306B1E9C3CC4E07A4D64E23FBDB232Candnm=Back+Issuesandtype=Publishingandmod=Publications%3A%3AArticleandmid=8F3A7027421841978F18BE895F87F791andtier=2anddid=9A6084AE4264441A9EC178DC96951FDCanddtxt=Vol%2E+3+No%2E+6+September+2003, [Last accessed on 2011 Apr 03].
11. Thangadurai S, Shukla SK, Srivastava AK, Anjaneyulu Y. X-ray powder diffraction patterns for certain fluoroquinolone antibiotic drugs. Acta Pharm 2003;53:295-303.
12. Choudhary D, Kumar S, Gupta GD. Enhancement of solubility and dissolution of glipizide by solid dispersion (kneading) technique. Asian J Pharmaceutics 2009;3:245-51.
13. Keraliya RA, Soni TG, Thakkar VT, Gandhi TR. Formulation and Physical characterization of microcrystals for dissolution rate enhancement of Tolbutamide. Int J Res Pharm Sci 2010;1:69-77.
14. Choi WS, Kwak SS, Kim HI. Improvement of bioavailability of water insoluble drugs: potential of nano-sized grinding technique. Asian J Pharm Sci 2006;1:27-30.
15. Nelson MP, Zugates CT, Treado PJ, Casuccio GS, Exline DL, Schlaegle SF. Combining raman chemical imaging and scanning electron microscopy to characterize ambient fine particulate matter. Aerosol Sci Technol 2001;34:108-17.
16. Lich BH, DesRosiers L, Elands J, Tinke AP, Sub Micron Particle Size and Shape Characterization by SEM; Available from:http://www.fei.com/uploadedFiles/DocumentsPrivate/Content/Sub_Micron_Particle_Sizeand_Shape_Chara cterization_by_SEM_2.pdf , [Last accessed on 2010 Jan 10].
17. Measurement Techniques for Nanoparticles; Available from: http://www.nanocap.eu/Flex/Site/Download.aspx?ID=3984, [Last accessed on 2010 Jan 04].
18. Inoue A. Determination of aspect ratios of clay-sized particles, Clay Science A. 1995;9:259-74.
19. Lich B. SEM-based systems can give researchers a better look at sub-micron Pharmaceutical particles; Available from: http://www.dddmag.com/article-SEM-BasedSystems020109.aspx, [Last accessed on 2010 Jan 20].
20. Venkeirsbilck T, Vercauteren A, Baeyens W, Weken GVD, Verpoort F, Vergote G, *et al*. Applications of raman spectroscopy in pharmaceutical analysis. Trends Anal Chem 2002;21:869-77.
21. Clarke RH, Londhe S, Premasiri WR, Womble ME. Low-resolution raman spectroscopy: Instrumentation and application in chemical analysis. J Raman Spectrosc 1999;30:827-32.
22. Silverstein RM, Webster FX. Spectrometric Identification of Organic Compounds. 6th ed. New York (USA): Jhon Wiley and Sons; 2002.
23. Dani VR. Organic Spectroscopy. 1st ed. New Delhi (India): Tata

McGraw-Hill Publishing Company Limited; 1995.

24. Precautions for Making KBr Pellets; Available from: http://www.chemistry.nmsu.edu/Instrumentation/KBr_New.html, [Last accessed on 2010 Jan 20].
25. Florence AJ, Kennedy AR, Shankland N, Wright E, Al-Rubayi A. Norfloxacin dehydrates. Acta Cryst 2000;56:1372-3.
26. Ramesh S, Ranganayakulu D, Reddy RSP, Tejaswi E. Formulation and evaluation of sepia nanoparticles containing ciprofloxacin hydrochloride. J Innovative Trends Pharm Sci 2010;1:79-85.
27. Tom RT, Suryanarayana V, Reddy PG, Baskaran S, Pradeep T. Ciprofloxacin protected gold nanoparticles. Langmuir 2004;20:1909-14.
28. Jiménez-Garrido N, Perello L, Ortiz R, Alzuet G, Alvarez MG, Canton E, *et al*. Antibacterial studies, DNA oxidative cleavage, and crystal structures of Cu(II) and Co(II) complexes with two quinolone family members, ciprofloxacin and enoxacin. J Inorg Biochem 2005;99:677-89.
29. Sharts DOSHCM, Gorelik VS. Method and apparatus for determination of carbon-halogen compounds and applications thereof. United States Patent 6445449; available from http://www.freepatentsonline.com/6307625.html, [Last accessed on 2011 Jan 20].
30. Raman Data and Analysis; Available from: http://www.horiba.com/fileadmin/uploads/scintific/Documents/Raman/bands.pdf, [Last accessed on 2010 Jan 20].
31. Tua Q, Eisenb J, Changa C. Band shifts in surface enhanced raman spectra of indolic molecules adsorbed on gold colloids; Available from: http://www.icors2010.org/abstractfiles/ICORS20101040.5375VER.5.pdf, [Last accessed on 2010 Jan 2].
32. Xu J, Stangel I, Butler IS, Gilson DF. An FT-Raman spectroscopic investigation of dentin and collagen surfaces modified by 2-Hydroxyethylmethacrylate. J Dent Res 1997;76:596-601.
33. Bright A, Devi TS, Gunasekaran S. Spectroscopical vibrational band assignment and qualitative analysis of biomedical compounds with cardiovascular activity. Int J Chem Tech Res 2010;2:379-88.
34. Skoulika SG, Georgiou CA. Rapid quantitative determination of ciprofloxacin in pharmaceuticals by use of solid-state FT-Raman spectroscopy. Appl Spectrosc 2001;55:1259-65.
35. Lawrence BA, Lei Z, Liling Z, Christopher LE, Andrew RB. Solid-state NMR analysis of fluorinated single - Carbon nanotubes: assessing the extent of fluorination. Chem Mater 2007;19:735-44.
36. Agarwal UP, Reiner RS, Pandey AK, Ralpha SA, Hirth KC, Atalla RH. Raman spectra of liginin model compounds; Available from: http://www.treesearch.fs.fed.us/pubs/20194, [Last accessed on 2010 Jan 20].
37. Precautions for Making KBr Pellets; Available from: http://www.chemistry.nmsu.edu/instrumentation/KBr_New.html, [Last accessed on 2010 Jan 20].
38. Gruodis A, Alkasa V, Powell DL, Nielsen CJ, Guirgis GA, Durig JR. Vibrational spectroscopic studies, conformations and ab initio calculations of 1,1,1 trifluoropropyltrifluorosilane. J Raman Spectrosc 2003;34:711-24.
39. Gupta SP. Statistical Methods. 18th ed. New Delhi (India): Sultan Chand and Sons; 2005.
40. Patel NK, Kennon L, Levinson RS. Pharmaceutical Suspensions. In: Lachman L, Lieberman HA, Kanig JL editors. The Theory and Practice of Industrial Pharmacy. 3rd ed. Bombay (India): Varghese Publishing House; 1991. p. 479-501.
41. Chouhan R, Bajpai A. Real Time *in vitro* studies of doxorubicin release from PHEMA nanoparticles. J Nanobiotechnology 2009;7:5.
42. Zhang X, Pan W, Gan L, Zhu C, Gan Y, Nie S. Preparation of a dispersible PEGylate nanostructured lipid carriers (NLC) loaded with 10-Hydroxycamptothecin by Spray-Drying. Chem Pharm Bull (Tokyo) 2008;58:1645-50.
43. Mortada I. The Influence of dosage Form on the bioavailability of Drugs Part 1, Principles of Gastro-Intestinal Drug Absorption Part 7, Available from: http://pharamcytimes.wordpress.com/2009/05/06/the-influence-of-the-dosage-form-on-the- bioavailability-of- drugs/, [Last accessed on 2010 Nov 20].
44. Boddupalli BM, Mohammed ZN, Ravinder NA, Banji D. mucoadhesive drug delivery system: An overview. J Adv Pharm Technol Res 2010;1:381-7.

How to cite this article: Sahoo S, Chakraborti CK, Mishra SC. Qualitative analysis of controlled release ciprofloxacin/carbopol 934 mucoadhesive suspension. J Adv Pharm Tech Res 2011;2:195-204.

Source of Support: Nil, **Conflict of Interest:** Nil.